

Supplementary information:

Janus nanoparticles designed for extended cell surface attachment

Reshma Kadam^a, Jaee Ghawali^a, Mario Waespy^b, Michael Maas^{a,c,}, Kurosch Rezwan^{a,c}*

**Corresponding author: email: michael.maas@uni-bremen.de, Tel. +49 421 218 – 64939,
Fax. +49 - 421 218 – 64932*

^a Advanced Ceramics, University of Bremen, Am Biologischen Garten 2, 28359 Bremen,
Germany

^b Center for Biomolecular Interactions Bremen and Centre for Environmental
Research and Sustainable Technology, Faculty 2 (Biology/Chemistry), University of
Bremen, Leobener Strasse, NW2, 28359 Bremen

^c MAPEX Centre of Materials and Processes, University of Bremen, 28359 Bremen,
Germany

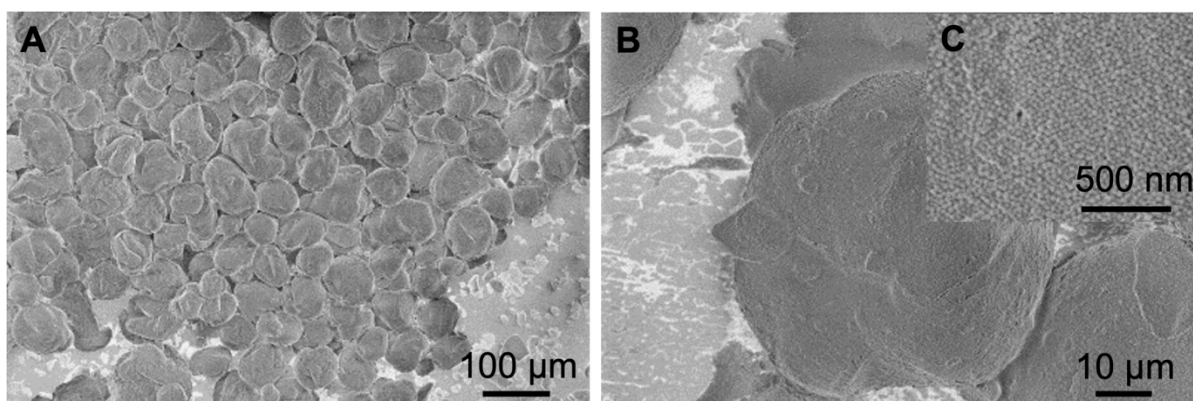


Fig.S1. SEM analysis of the wax Pickering emulsion droplets prepared using APTES functionalized RBITC-SiO₂ Janus nanoparticles. **(A)** overview of the wax droplets, **(B)** closeup of a single wax droplet and **(C)** nanoparticles on the droplet surface from **(B)**.

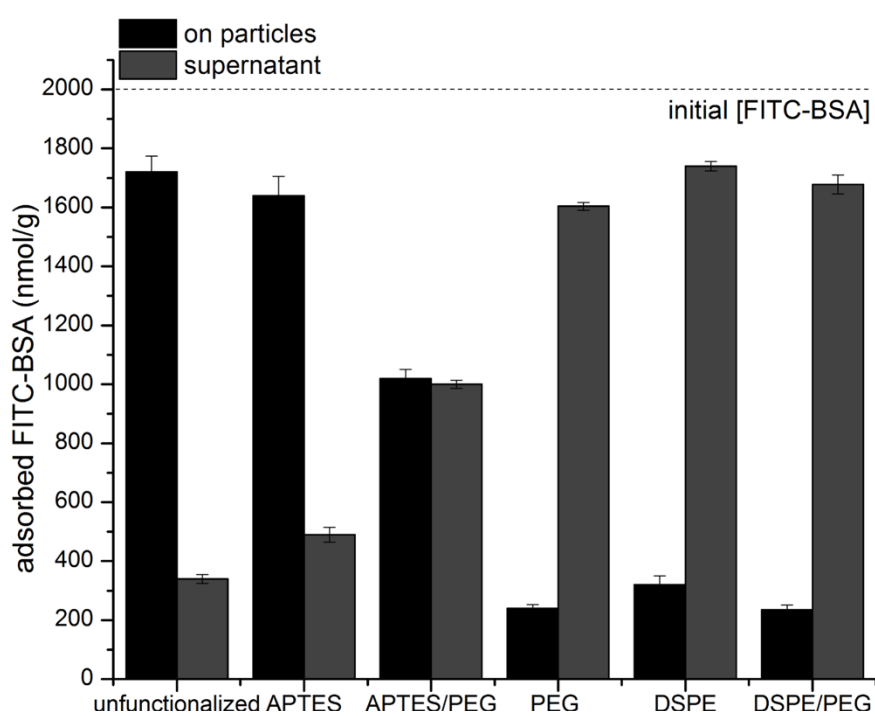


Fig.S2. Confirmation of the presence of PEG groups by quantification of adsorbed FITC-BSA. The amount of adsorbed FITC-BSA on the nanoparticles was quantified using fluorescence spectroscopy. The total amount of FITC-BSA in each case was 2000 nmol/g of nanoparticle.

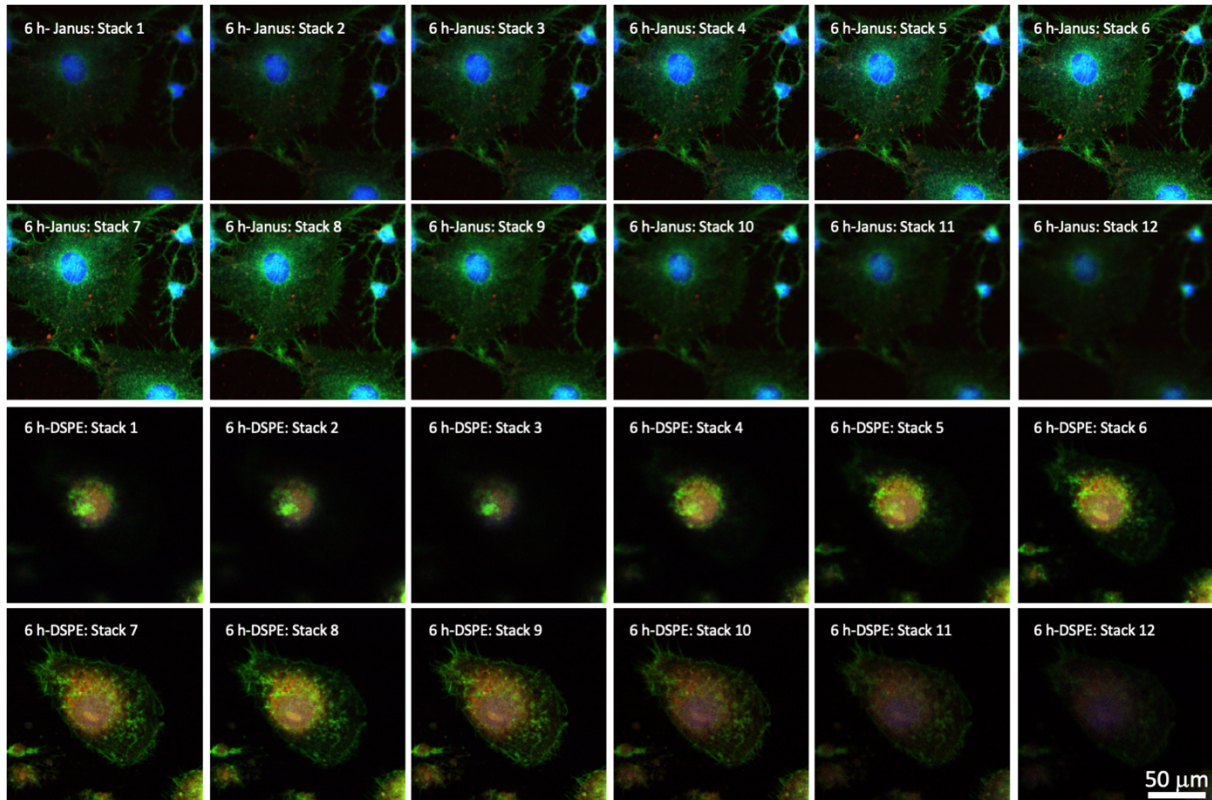


Figure S3: Representative Z-stack CLSM images of NIH 3T3 cells after incubation with DSPE/PEG Janus and DSPE particles for 6 h. The distance between the stack images is 200 nm with the first stack corresponding to the top of the cell and the last to the bottom. The nuclei were stained using DAPI (blue), the cytoskeleton was dyed with AF-488 conjugated phalloidin (green) and the nanoparticles were labelled with RBITC (red).

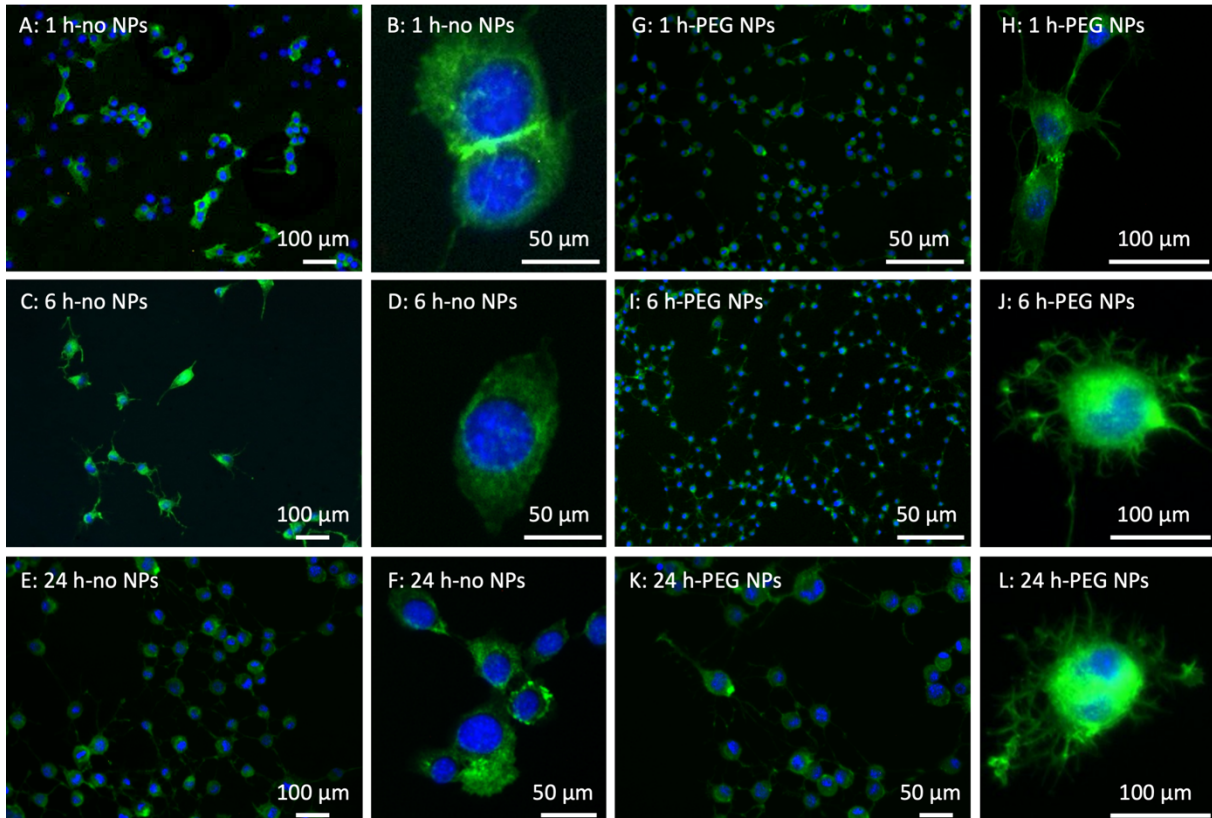


Fig. S4. Fluorescence microscopy (A, C, E, G, I K) and laser scanning confocal microscopy (B, D, F, H, J, L) of NIH 3T3 cells before and after exposure of the fully PEG functionalized nanoparticles. The cells were incubated with PEG functionalized nanoparticles for 1 h, 6 h and 24 h followed by fluorescence staining with specific fluorescent dyes. The merged images were recorded using the DAPI-, FITC- and RBITC- channels. The nuclei and cytoskeletons were stained using the dyes DAPI and AF-488 conjugated phalloidin respectively, whereas the nanoparticles have been labelled with RBITC.

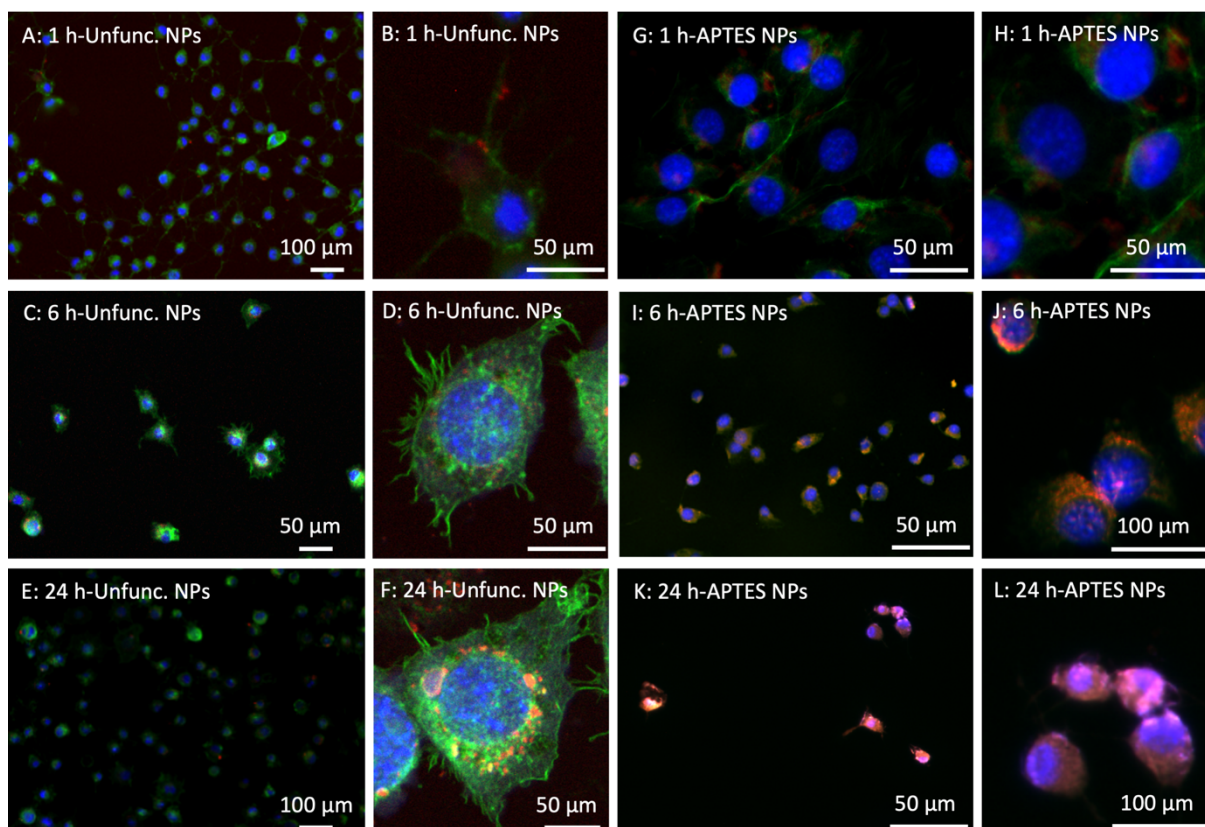


Fig. S5. Fluorescence microscopy (A, C, E, G, I K) and laser scanning confocal microscopy (B, D, F, H, J, L) of NIH 3T3 cells after exposure of the unfunctionalized and APTES functionalized nanoparticles. The cells were incubated with the respective nanoparticles for 1 h, 6 h and 24 h followed by fluorescence staining with specific fluorescent dyes. The merged images were recorded using the DAPI-, FITC- and RBITC- channels. The nuclei and cytoskeleton were stained using the dyes DAPI and AF-488 conjugated phalloidin respectively, whereas the nanoparticles have been labelled with RBITC.

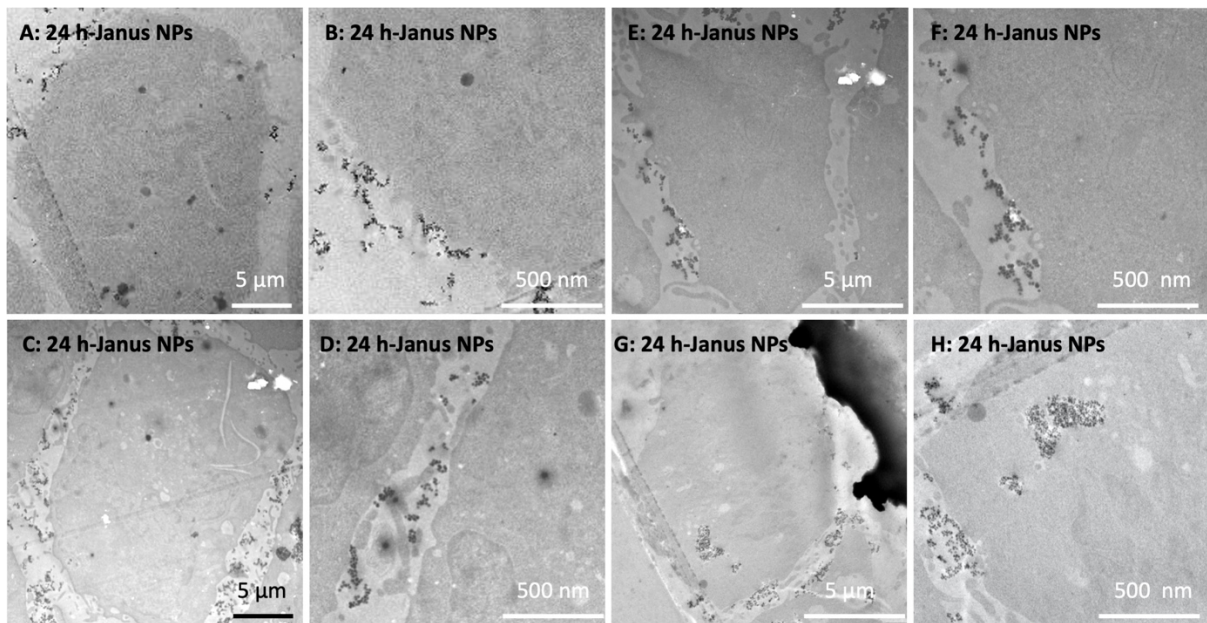


Fig. S6. TEM of the NIH 3T3 cells after incubation with DSPE/PEG (Janus) RBITC SiO₂ nanoparticles for 24 h. The images of the second and fourth column are higher magnifications of the images of the first and third row, respectively. Each sample was first embedded in epoxy resin followed by preparing ultrathin microtome sections of up to 50 nm thickness followed by TEM analysis.

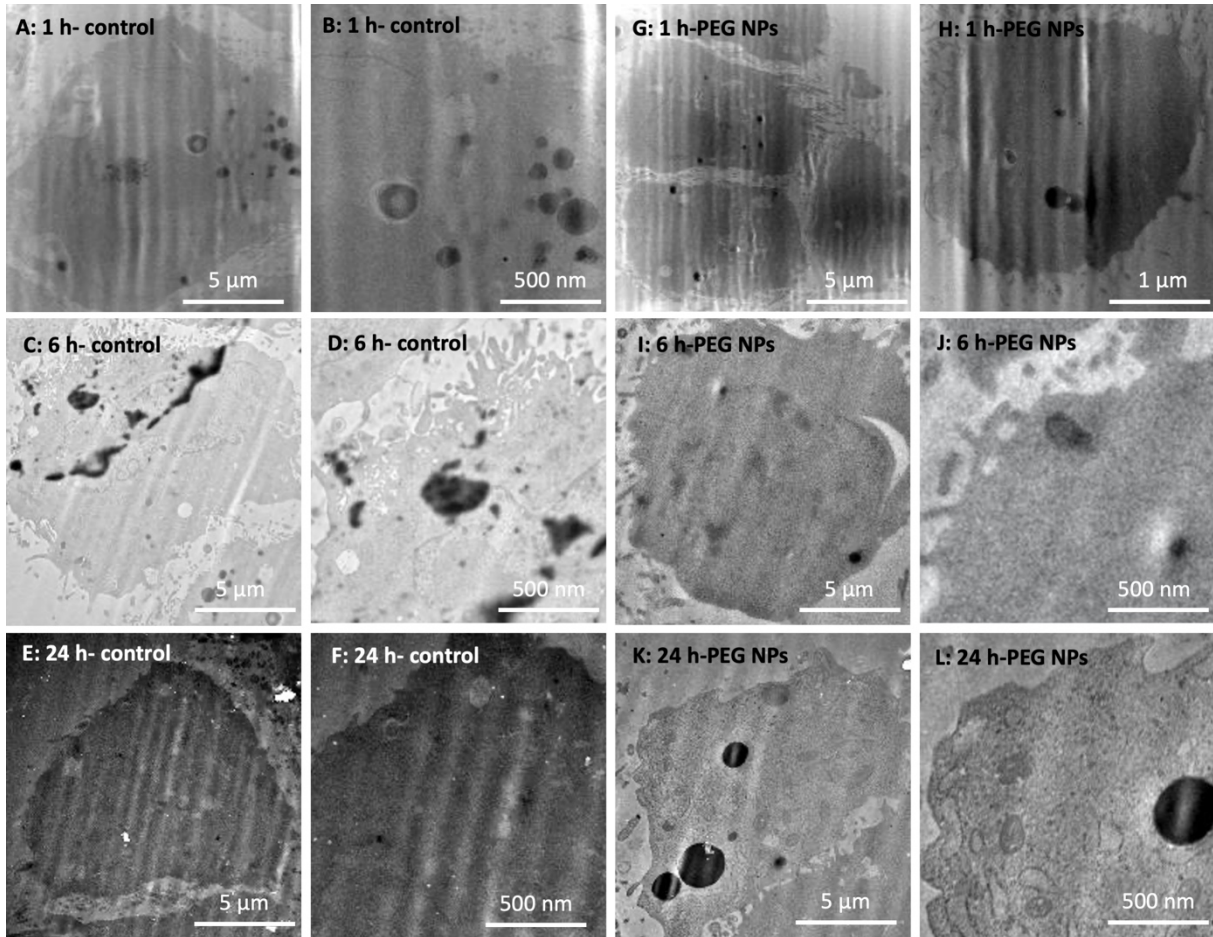


Fig. S7. TEM of the NIH 3T3 cells after incubation without (control) and with PEG nanoparticles for 1 h, 6 h and 24 h. The images of the second and fourth column are higher magnifications of the images of the first and third row, respectively. Each sample was first embedded in epoxy resin followed by preparing ultrathin microtome sections of up to 50 nm thickness followed by TEM analysis.

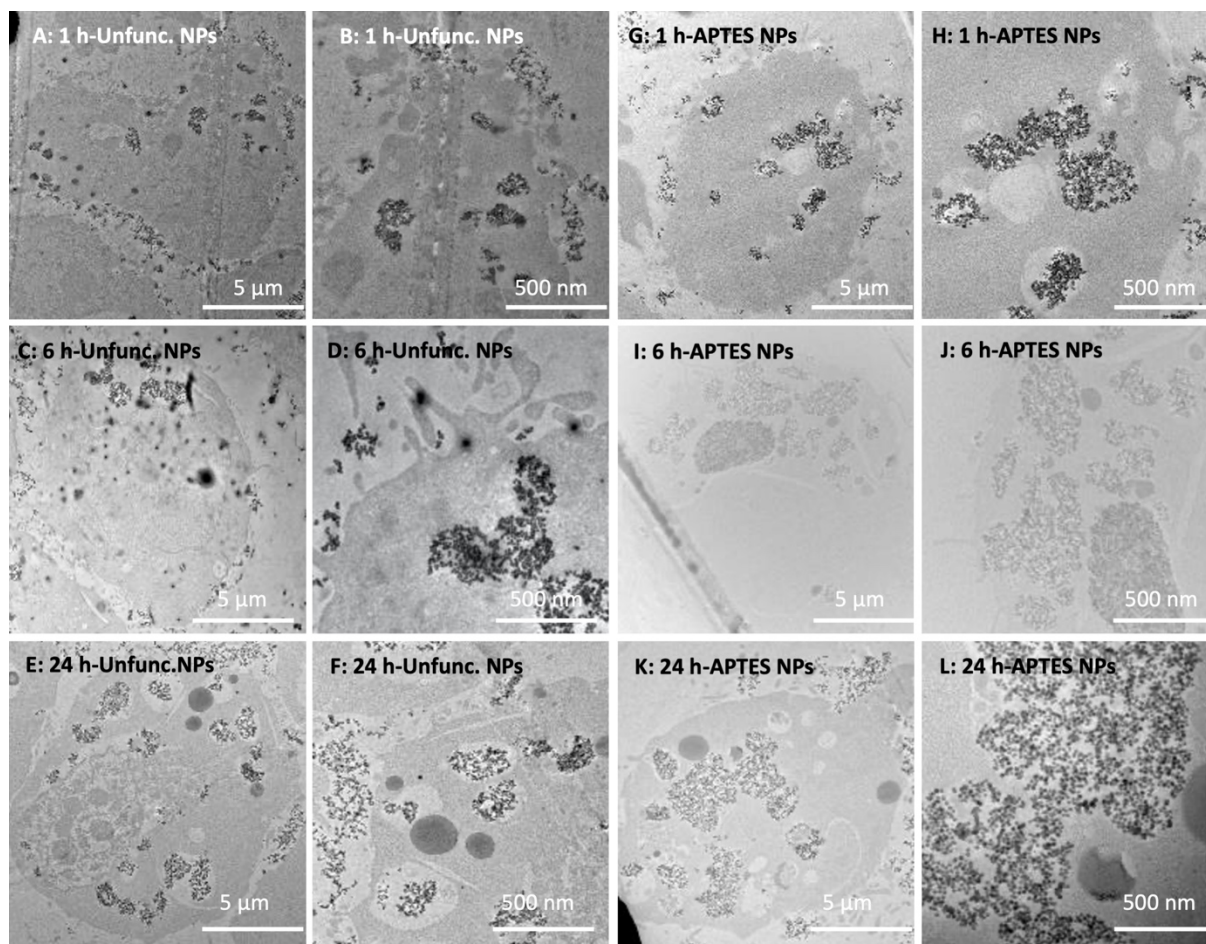


Fig. S8. TEM of the NIH 3T3 cells after incubation with unfunctionalized and APTES nanoparticles for 1 h, 6 h and 24 h. The images of the second and fourth column are higher magnifications of the images of the first and third row, respectively. Each sample was first embedded in epoxy resin followed by preparing ultrathin microtome sections of up to 50 nm thickness followed by TEM analysis.

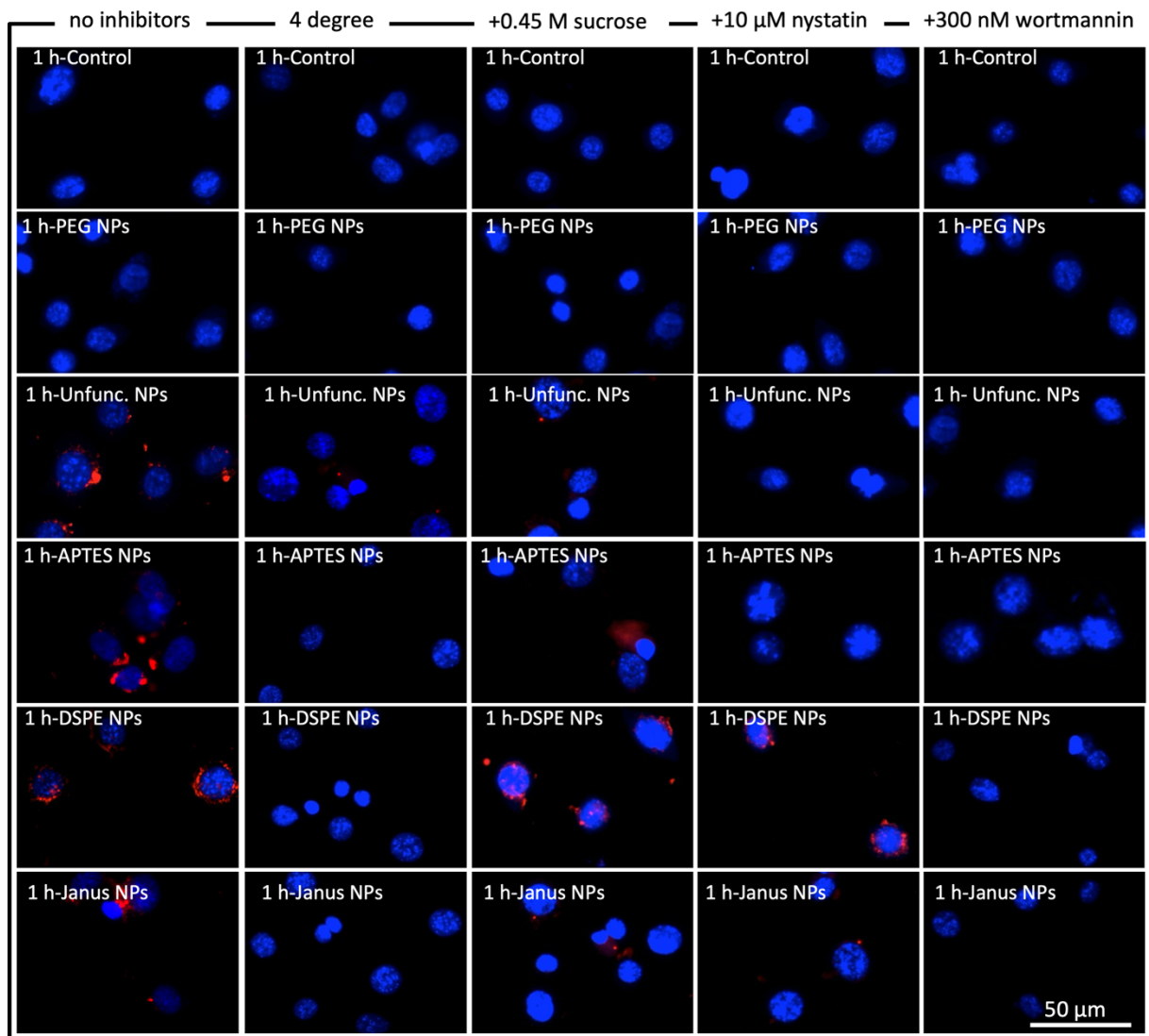


Fig. S9. Fluorescence microscopy of NIH 3T3 cells before (control) and after exposure of the different nanoparticles for 1 h in the presence and absence of endocytosis inhibitors. 4 °C incubation was performed to suppress temperature-dependent endocytosis, hypertonic sucrose suppressed receptor-mediated endocytosis, nystatin inhibits caveolae-mediated endocytosis and wortmannin inhibits macropinocytosis. The nuclei were stained using DAPI (blue), whereas the nanoparticles were labelled with RBITC (red).

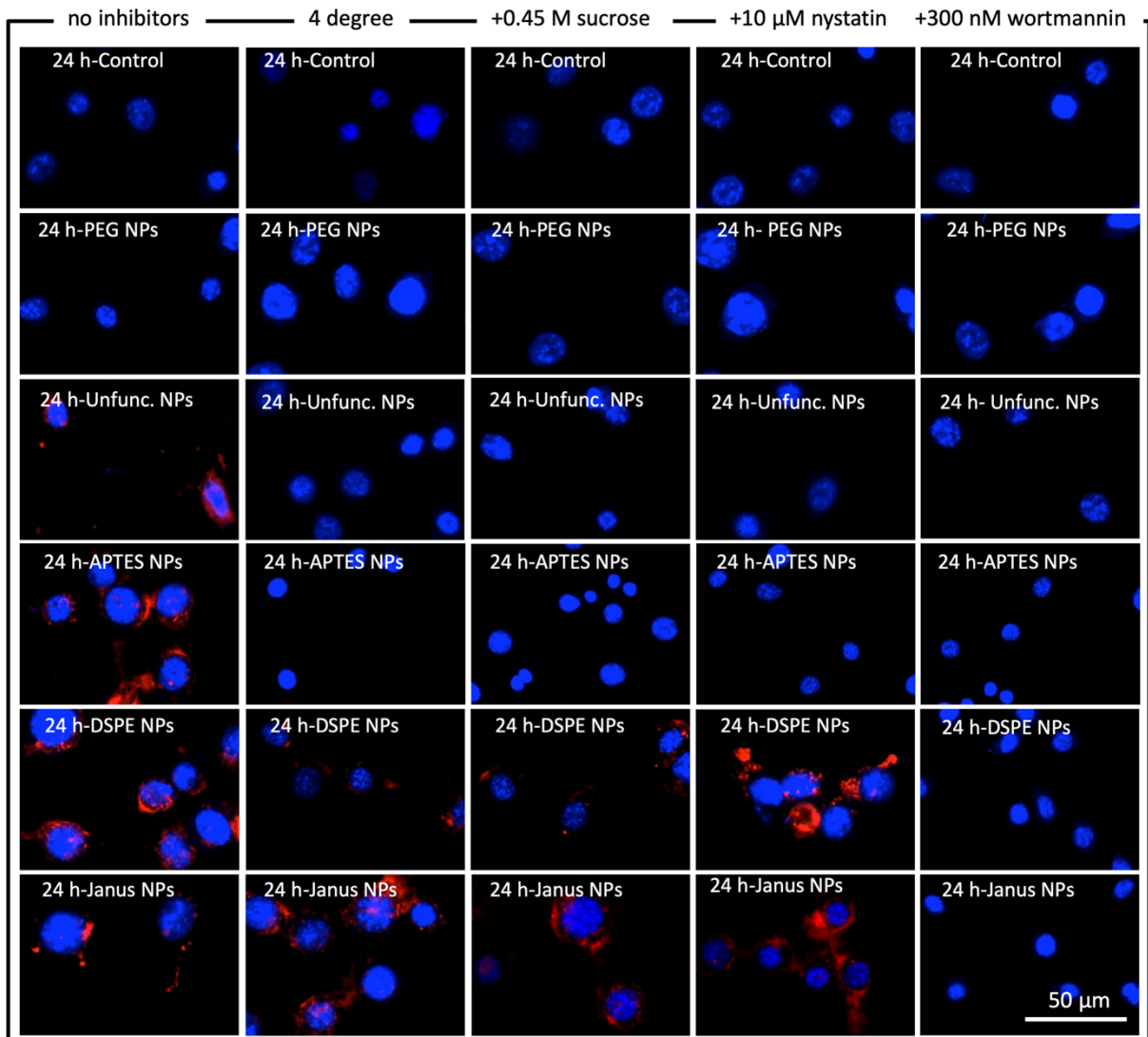


Fig. S10. Fluorescence microscopy of NIH 3T3 cells before (control) and after exposure of the different nanoparticles for 24 h in the presence and absence of endocytosis inhibitors. 4 °C incubation was performed to suppress temperature-dependent endocytosis, hypertonic sucrose suppressed receptor-mediated endocytosis, nystatin inhibits caveolae-mediated endocytosis and wortmannin inhibits macropinocytosis. The nuclei were stained using DAPI (blue), whereas the nanoparticles were labelled with RBITC (red).

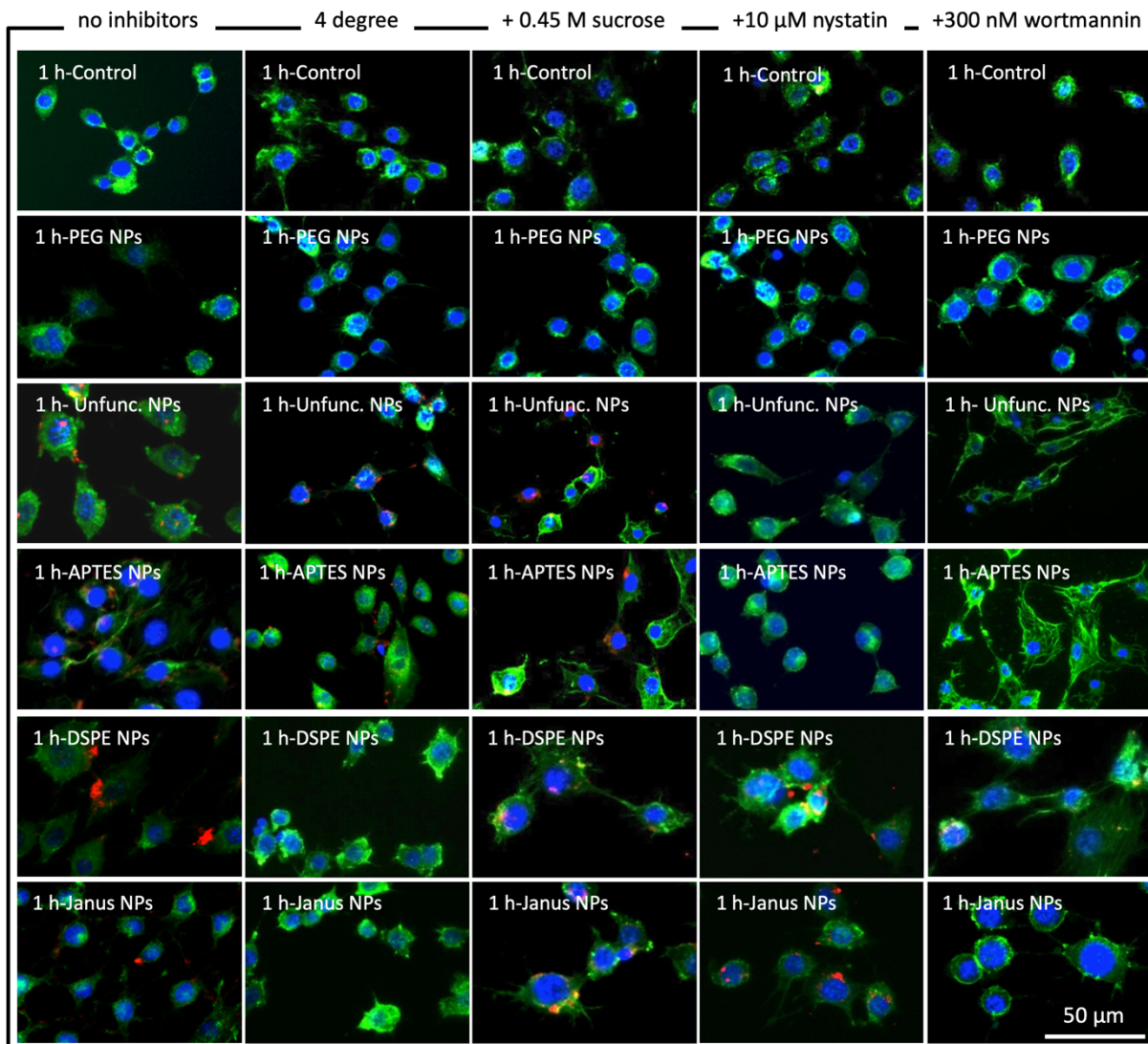


Fig. S11. Fluorescence microscopy of NIH 3T3 cells before (control) and after exposure of the different nanoparticles for 1 h in the presence and absence of endocytosis inhibitors. 4 °C incubation was performed to suppress temperature-dependent endocytosis, hypertonic sucrose suppressed receptor-mediated endocytosis, nystatin inhibits caveolae-mediated endocytosis and wortmannin inhibits macropinocytosis. The nuclei were stained using DAPI (blue), the cytoskeleton was dyed with AF-488 conjugated phalloidin (green) and the nanoparticles were labelled with RBITC (red).

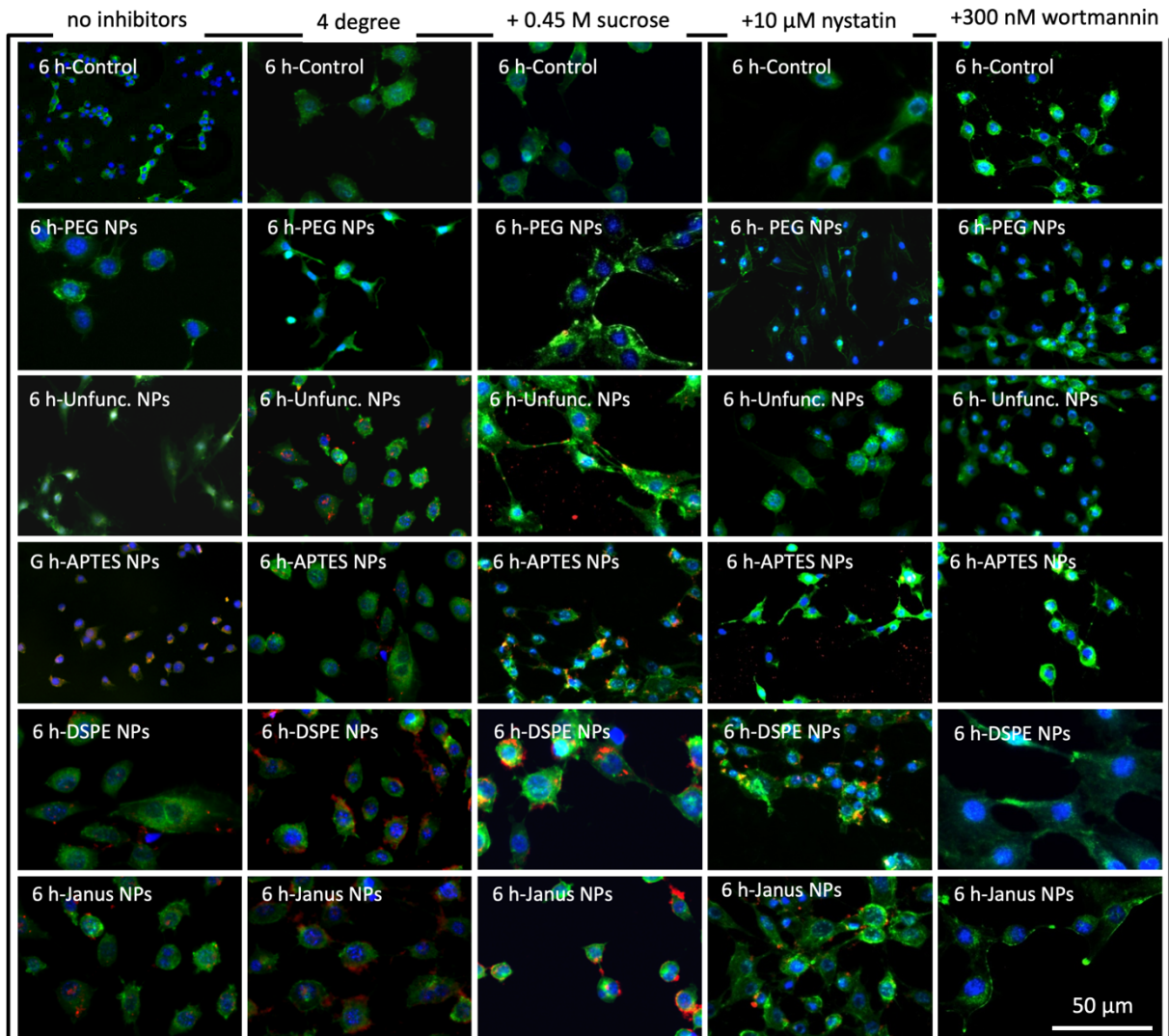


Fig. S12. Fluorescence microscopy of NIH 3T3 cells before (control) and after exposure of the different nanoparticles for 6 h in the presence and absence of endocytosis inhibitors. 4 °C incubation was performed to suppress temperature-dependent endocytosis, hypertonic sucrose suppressed receptor-mediated endocytosis, nystatin inhibits caveolae-mediated endocytosis and wortmannin inhibits macropinocytosis. The nuclei were stained using DAPI (blue), the cytoskeleton was dyed with AF-488 conjugated phalloidin (green) and the nanoparticles were labelled with RBITC (red).

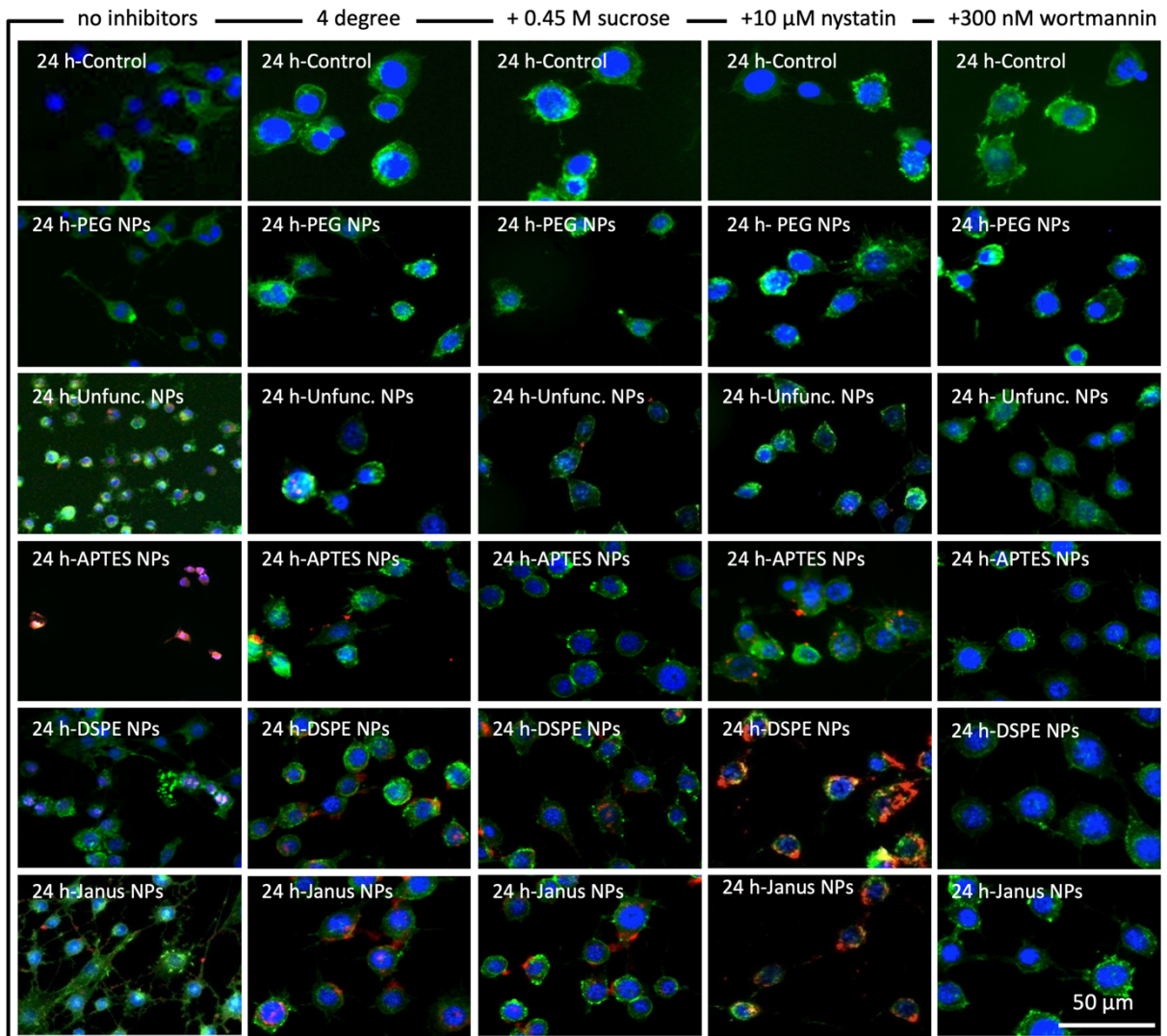


Fig. S13. Fluorescence microscopy of NIH 3T3 cells before (control) and after exposure of the different nanoparticles for 24 h in the presence and absence of endocytosis inhibitors. 4 °C incubation was performed to suppress temperature-dependent endocytosis, hypertonic sucrose suppressed receptor-mediated endocytosis, nystatin inhibits caveolae-mediated endocytosis and wortmannin inhibits macropinocytosis. The nuclei were stained using DAPI (blue), the cytoskeleton was dyed with AF-488 conjugated phalloidin (green) and the nanoparticles were labelled with RBITC (red).

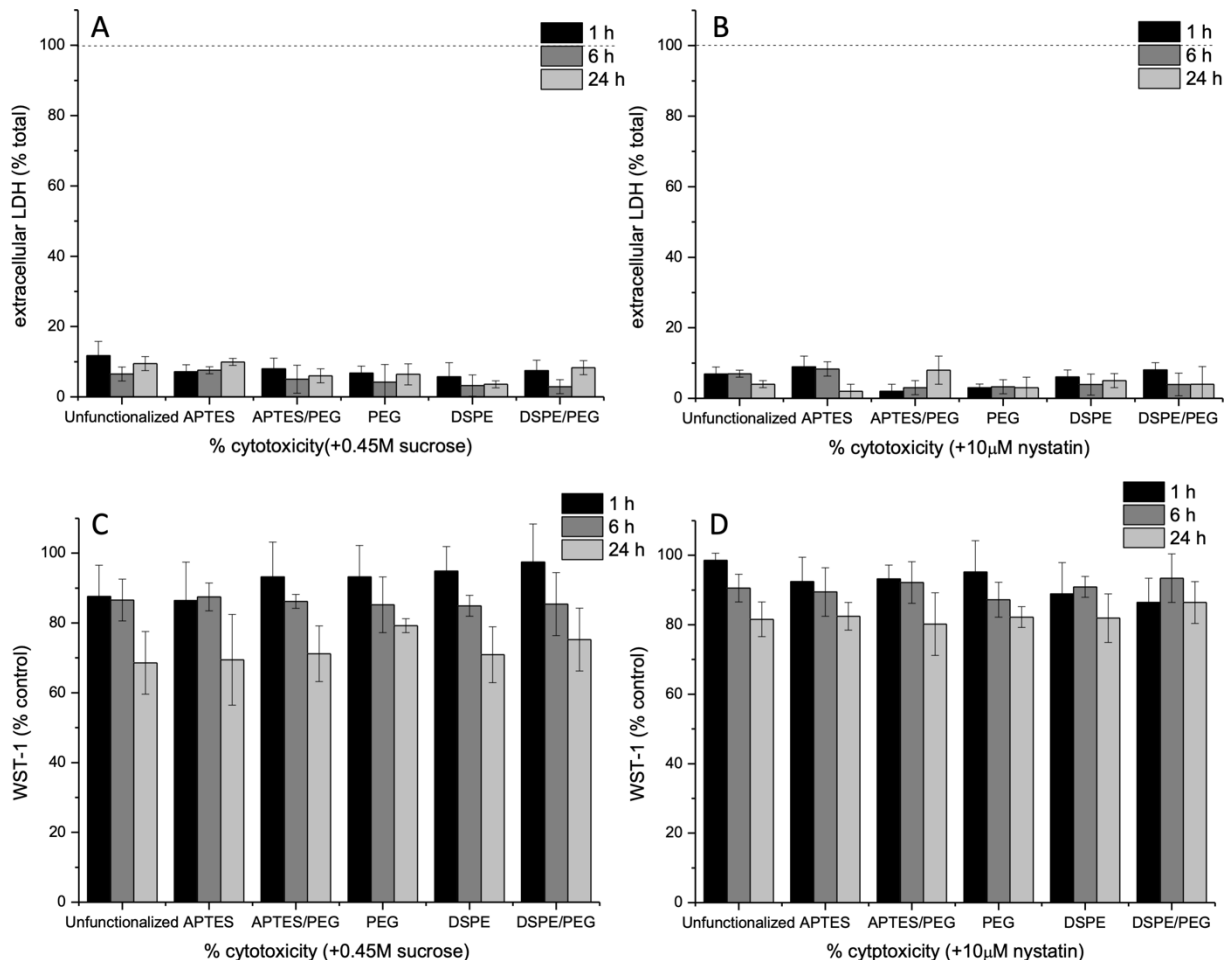


Fig. S14. Cell viability after incubation with different nanoparticle types in the presence hypertonic sucrose and nystatin for 1h, 6 h and 24 h. Membrane integrity was measured via the LDH assay (**A, B**) and mitochondrial viability was assessed using the WST-1 assay (**C, D**).